CONF-801111--53

DE82 004089

SINGLE AND MULTIPLE ELECTRON LOSS PROCESSES IN MeV HEAVY ION-TARGET COLLISIONS

G. D. Alton*

Physics Division, Oak Ridge National Laboratory, Oak Ridge, TN 37830

Summary

Experimental data, derived from the study of interactions between MeV heavy ions and gaseous targets are presented which illustrate important physical aspects such as the dependence of cross sections on projectile velocity, and projectile and target atomic numbers. Included are data which reflect the importance of the electron binding energy, the existence of shell effects, the possibility of target polarizability, and the presence of non-additivity and density effects in electron loss processes. Charge state yield versus scattering angle, a prescription for relating total single electron loss cross section per atom atomic and molecular target data and formulas which predict electron loss cross sections with reasonable accuracy are also given.

Introduction

Theoretical and experimental studies of collisional processes which occur during interactions of high energy particles with matter has provided much of the fundamental information which has led to our present understanding of atomic systems and atomic system structures. Such investigations have continually progressed since the pioneering work of Thompson and Rutherford.

During passage through matter, a heavy ion loses and captures electrons in successive collisions which leads to a statistical distribution of charge states in an ion beam. At low pressures, the distribution varies with target thickness until charge state equilibrium is established. The study of such processes under single collision conditions (thin targets) can yield fundamental information about such interactions. Equilibrium charge state distributions are established in thicker targets which involve multiple collisions and information there about is of considerable practical importance to the accelerator user who benefits by the disparity between multiple electron loss and capture processes as a means of increasing the beam intensity in a given charge state.

A rather extensive amount of data has been accumulated on the latter subject by several experimental groups much of which is included in the review articles by Nikolaev,[1] Betz,[2] and Moak.[3,4] Many studies such as those of Datz *et al.*,[5] Alton *et al.*,[6] Moak *et al.*,[7] and Knudsen *et al.*[8] also contain information concerning equilibrium and non-equilibrium charge changing processes. From these data and the empirical formulations of Nikolaev and Dimitriev[9] and Sayer[10] most of the present day accelerator related charge state information can be computed for a variety of projectiles, projectile energies, and target combinations.

As a result of such collisional processes, the energy of the ion beam gradually degrades. Considerable efforts have been made by several experimental groups toward improving the understanding of the basic energy loss mechanisms which take place as heavy particles penetrate matter. Projectile energy losses at energies below nuclear excitation levels are attributable to elastic nuclear and electronic encounters, discrete electronic excitations accompanied by radiation, and electron capture and loss processes. The relative importance of the particular mechanism depends on the velocity of the particle in the medium in which it passes. Projectile capture and loss at projectile velocities of the order of the orbital velocities of the electrons being captured or removed are important energy transfer processes which are readily accessible experimentally through measurement of the relevant cross sections.

The physics of high energy ion-atom collisions can best be understood when studies are conducted under single event conditions and where differential and total scattering information can be extracted from measurements without ambiguity. This criterion dictates the use of dilute gaseous targets because of the very high densities associated with solid targets in which single event conditions cannot be easily met.

In order to effect an understanding of electron loss processes, many parametric studies must be made including their dependence on projectile, projectile atomic number Z_1, projectile energy E or velocity v, projectile incident charge state q_i, and atomic number of the target Z_2. Many investigations have been made of charge changing processes with a variety of ions at specific energies and initial charge states. Review articles on the subject have been published by Allison,[11] Allison and Garcia-Munoz,[12] and Northcliffe,[13] as well as by Nikolaev[1] and Betz.[2] Several studies emphasize energy or velocity dependence of the charge changing interactions (e.g. Macdonald and Martin,[14] Macdonald *et al.*,[15] Ferguson *et al.*,[16] and Tonuma *et al.*[17] while other studies emphasize other parameters such as target atomic number (Knudsen *et al.*[8] and Alton *et al.*[18]).

The relation between charge state yield or differential scattering cross section and scattering angle is fundamental to the understanding of the dynamics of collisional processes. A few measurements have been made of scattering processes under single event conditions such as those reported by Kessel,[19] Spicuzza and Kessel,[20] Alton *et al.*,[6] Bridwell *et al.*,[21] and Scott *et al.*[22]

The complexity of interactions between high velocity multielectron projectiles and various types of targets has precluded accurate theoretical descriptions of electron loss processes. However, the theoretical developments of Bohr[23] and Bohr and Lindhard[24] have provided qualitative descriptions of charge changing phenomena in high energy heavy projectile target interactions which today serve as useful guidelines for estimating cross sections and understanding the physical processes involved in such collisions. The difficulty of an accurate analysis is readily apparent when one considers the very large number of electronic configurations which are possible in such interactions.

In the present paper, selected data from the literature will be presented which illustrate important aspects of electron loss cross sections for high energy heavy ions traversing gaseous targets. The rather extensive amount of data which has been accumulated on

*Research sponsored by the U.S. Department of Energy, Division of Basic Energy Sciences under Contract No. W-7405-eng-26 with Union Carbide Corporation.

MF(i)

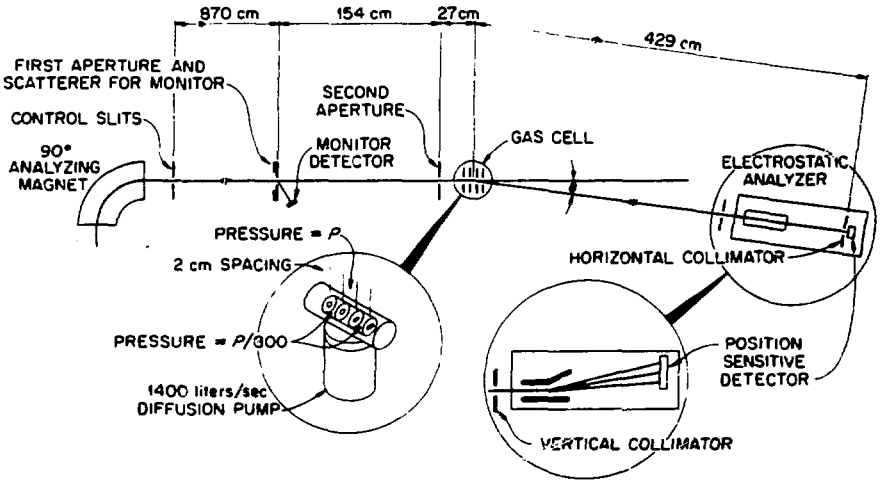

Fig. 1. Experimental arrangement for high angular resolution scattering measurements (ORNL).

the subject and the requirement of brevity, necessarily limits the amount of data presented and their discussions. The reader is referred to the review articles cited and other included references for more comprehensive information.

Scattering Studies

The study of the scattering of high energy heavy ions from specific targets can provide detailed information concerning the physics of such interactions. A limited number of such experiments involving MeV heavy ions has been reported in the literature. The correlation of charge state yield or differential scattering cross section with scattering angle can be of fundamental importance in understanding the dynamics of these interactions and of practical importance to the accelerator engineer in the design of terminal strippers for these devices.

The Experimental Arrangement. Various experimental arrangements have been used in scattering experiments such as described by Ryding *et al.*[25] and Kessel.[24] In order to be able to study processes which result in scattering of particles through very small angles, a high angular resolution experimental arrangement is desirable. The arrangement used at Oak Ridge National Laboratory in such experiments is shown in Fig. 1. The system has been described previously by Alton *et al.*[6] The device consists of a beam collimation system for defining a momentum analyzed ion beam of prescribed energy and charge state, a beam monitor system for measuring the intensity of the ion beam used in the experiment, a differentially pumped gas cell into which target gases are introduced, an electrostatic charge state analyzer for dispersing beams of differing charge which are formed during collisions in the target, and a position sensitive detector for counting the particles of a given charge state. The beam monitor consists of a thin annular nickel film surrounding an aperture which scatters a portion of the incident beam onto a surface barrier detector. The monitor detector serves as an indicator of the primary beam which enters the target when calibrated against the beam signal which strikes a detector mounted after the gas cell at the end of the apparatus. The calibration is made with no gas in the cell, so that the monitor serves as an indirect real-time indicator of the number of primary particles passing through the target at all times during the scattering measurement. In this way absolute differential charge state yields as a function of scattering angle are readily determined from a knowledge of the target thickness $t = n_o \times (\#/cm^2)$ where n_o is the density of target atoms and x is the cell length. The cell pressure in this arrangement is monitored with a standard capacitance manometer with set point feedback control system. The gas cell serves as the pivot point about which the beam line and charge state analysis and detection systems can be rotated. The system has a nominal angular resolution of $\Delta\theta = 0.054°$ with a solid angle subtended from the center of the cell of 2.4×10^{-7} ster.

A set of angular distributions of the charge states produced in collisions between 20 MeV I^{+6} and Ar (cell: length: 2 cm; cell pressure: 5×10^{-3} Torr) is shown in Fig. 2 which were measured by Alton *et al.*[6] using the previously discussed apparatus. The data illustrate the so-called "hollow beam" effect in that high charge state ions which are produced in more violent low impact parameter collisions exhibit maxima at non-zero scattering angles. Similiar effects have been observed by Ryding *et al.*,[25] Kessel,[19] and Spicuzza and Kessel.[20] Differential scattering cross sections produced in collisions between 60 MeV I^{10+} and Xe are shown to vary, as expected, with the number of electrons removed in the collision (Bridwell *et al.*[21]). A plot of differential cross section versus number of electrons removed is shown in Fig. 3. Integration over angle produced total electron loss cross sections ranging from 1.9×10^{-18} cm^2 for $\Delta q = 14$ to 1.6×10^{-17} cm^2 for $\Delta q = 11$.

Differential charge state yield or differential cross section data offer a means of testing various scattering potential models by using classical scattering theory. Experimental scattering data obtained from measurements of the absolute differential charge state yields from interactions of 20 MeV Cl^{4+} and I^{3+} ions with gaseous targets have been analyzed in terms of the impact parameters involved in such collisions by Scott *et al.*[22] A set of the yield data versus Thomas-Fermi impact parameter for 20 MeV I^{3+} and Ar target gas is shown in Fig. 4.

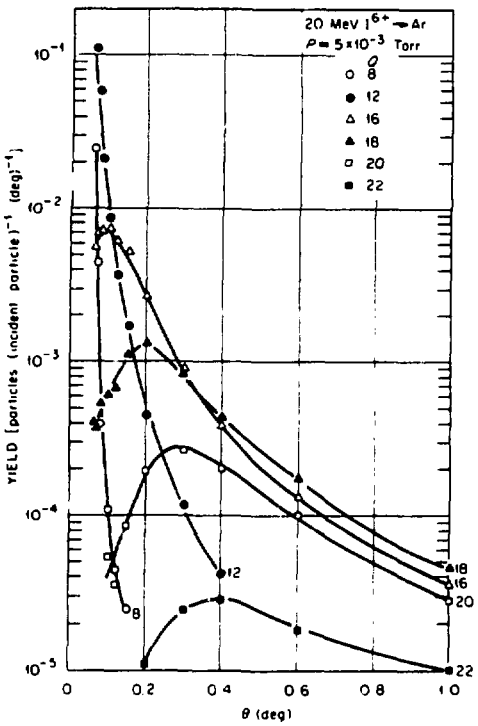

Fig. 2. Charge state yields vs. angle 20 MeV I^{6+} ions. (Pressure - .005 Torr; cell length - 2 cm) (Alton *et al.*[6])

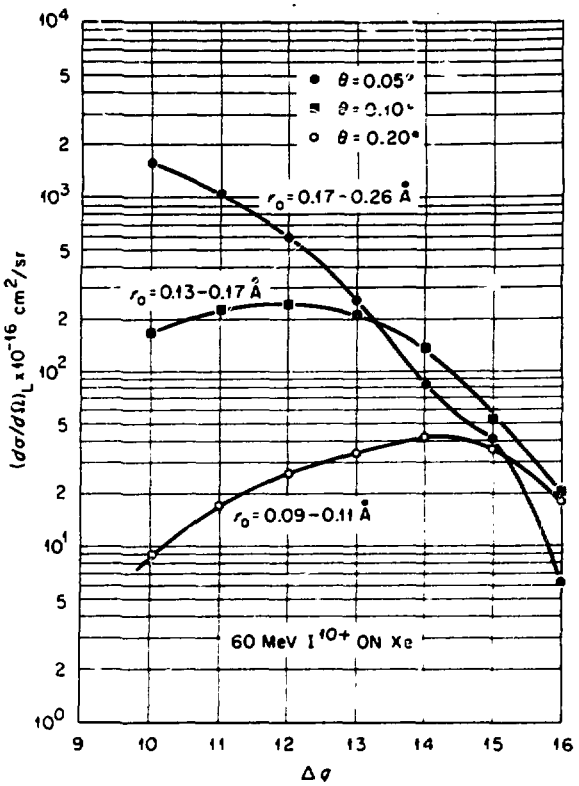

Fig. 3. Differential scattering cross sections for the removal of Δq electrons in single collisions between 60 MeV I^{10+} and Xe. (Bridwell *et al.*[21])

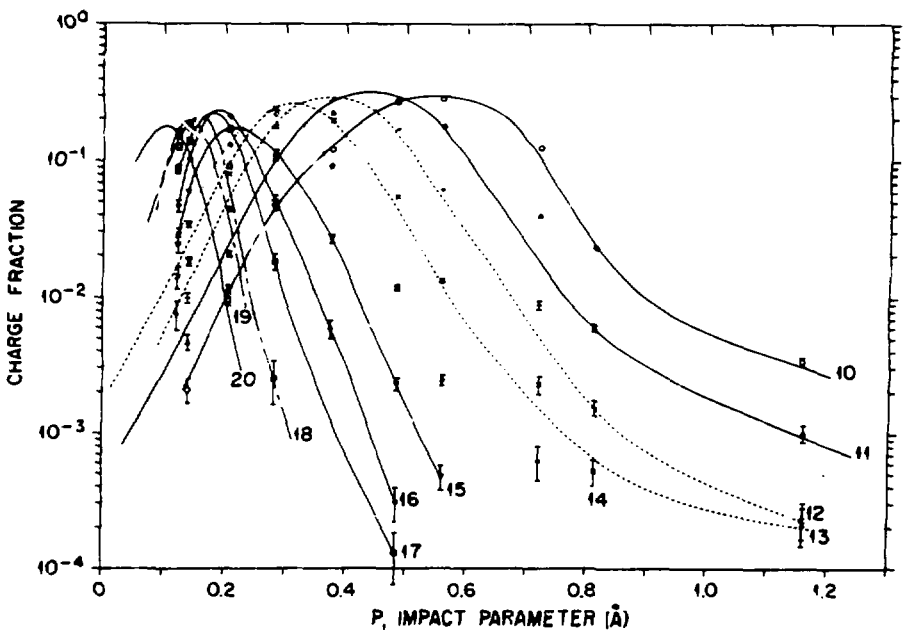

Fig. 4. Charge state fractions vs. Thomas-Fermi impact parameter for 20 MeV $^{127}I^{5+}$ incident on Xe (5 mTorr, 2 cm gas cell). $10 \geq q \geq 20$. Bars indicate statistical uncertainties. (Scott *et al.*[22])

Comparisons between measured total electron loss versus final projectile charge state and those calculated by use of Bohr, Thomas-Fermi and Lenz-Jensen potentials are shown in Fig. 5. We note that the measured values almost always are higher than those computed from the respective potentials indicating their inadequacies for properly representing such interactions. Analyses such as those described above offer a means of developing more appropriate scattering potentials for these processes.

Total Electron Loss Cross Section Measurements

Experimental Arrangement. Several experimental arrangements have been discussed in the previously cited literature for determining electron loss cross sections. The apparatus used at Oak Ridge National Laboratory differs from most in that it incorporates a lens for effectively integrating over all scattering angles. The lens greatly simplifies and facilitates data accumulation in such experiments. The apparatus, shown schematically in Fig. 6, has been described in detail by Moak *et al.*[7] previously and therefore only the salient features will be repeated here. The projectile and energy of interest produced in the ORNL EN tandem electrostatic accelerator is momentum analyzed, and collimated to a diameter of 1/2 mm immediately before entering a differentially-pumped gas cell. After emerging from the cell, individual charge states, from the multiplicity of states produced during projectile passage through the target, are focused by means of the magnetic quadrupole doublet lens through an electrostatic charge state analyzer and onto a position sensitive detector. All components in the system are precisely aligned and tested with the ion beam in order to ensure that no losses occur during beam transit to the detection system due to quadrupole steering or component misalignment. Prior to data accumulation, quadrupole setting are determined for each charge state in order to assure the simultaneous detection of all particles of the particular focussed charge state, while maintaining good spatial resolution between adjacent charge states. The arrangement permits fast data accumulation since several charge states can be totally collected. Cell pressures are measured with a standard capacitance manometer and feedback control system.

The Velocity Dependence of Electron Loss. Among the questions to be answered concerning electron loss processes is, how do they depend on projectile velocity, projectile, and target atomic numbers? Several experimental investigations have been made which address these questions and data exist which suggest general trends in loss cross section versus these parameters.

According to theoretical predictions of Bohr and Lindhard,[24] single electron loss cross sections are expected to maximize at projectile velocities v close to the velocity of the electron being removed or $v = \gamma u$ where γ is a constant near unity and increases slightly with target atomic number. Verifications of this prediction have been made by Nikolaev,[1] Macdonald *et al.*,[15] Ferguson *et al.*,[16] and Tonuma *et al.*[17] for a few projectile-target combinations. Sets of data taken from the work of Nikolaev and Macdonald *et al.* are shown in Figs. 7 and 8, respectively. The data of Nikolaev (Fig. 7) were measured with ion beams of helium and nitrogen in He targets. The incident charge states used in the measurements are indicated by each curve. For these measurements, the value of γ was found to be 1.35. The data of Macdonald *et al.*, shown in Fig. 8 for F^{q+} ions passing through nitrogen targets, include both single and multiple electron loss cross section results. The experimenters obtained γ values ranging from ~1 to 2 for a number of single electron loss cross sections. Multiple electron loss data versus ion velocity as observed by Macdonald and Martin[14] for O^{q+} ions and F^{q+} by Macdonald *et al.* ions in N_2 targets for cross sections leading to the same final charge state are found to be qualitatively similiar. These

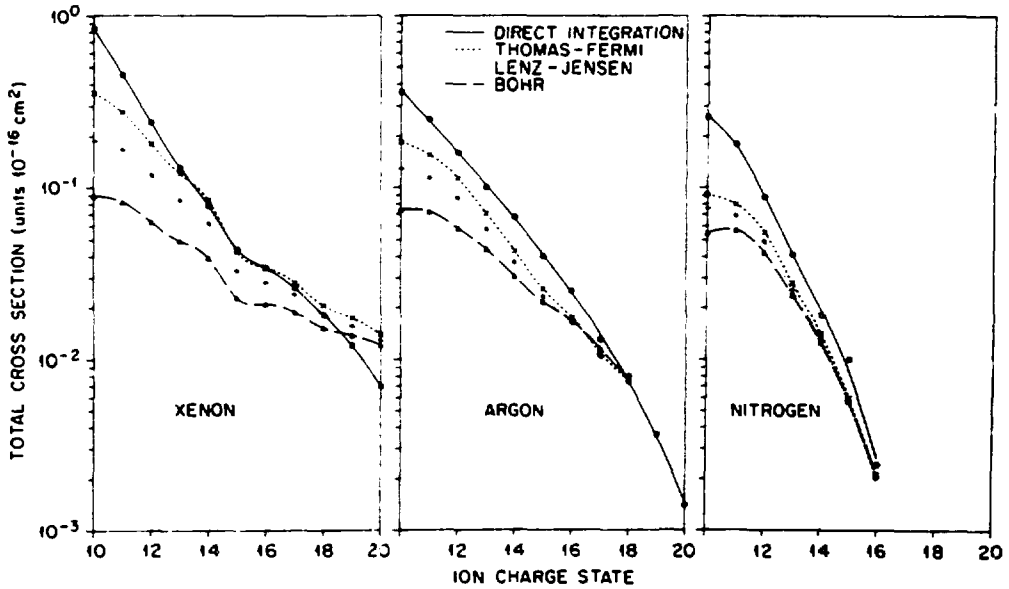

Fig. 5. Electron loss cross sections $\sigma(5,q)$ for 20 MeV $^{127}I^{5+}$ on Xe, Ar, and N_2. Symbols refer to means of determining cross sections. (Scott *et al.*[22])

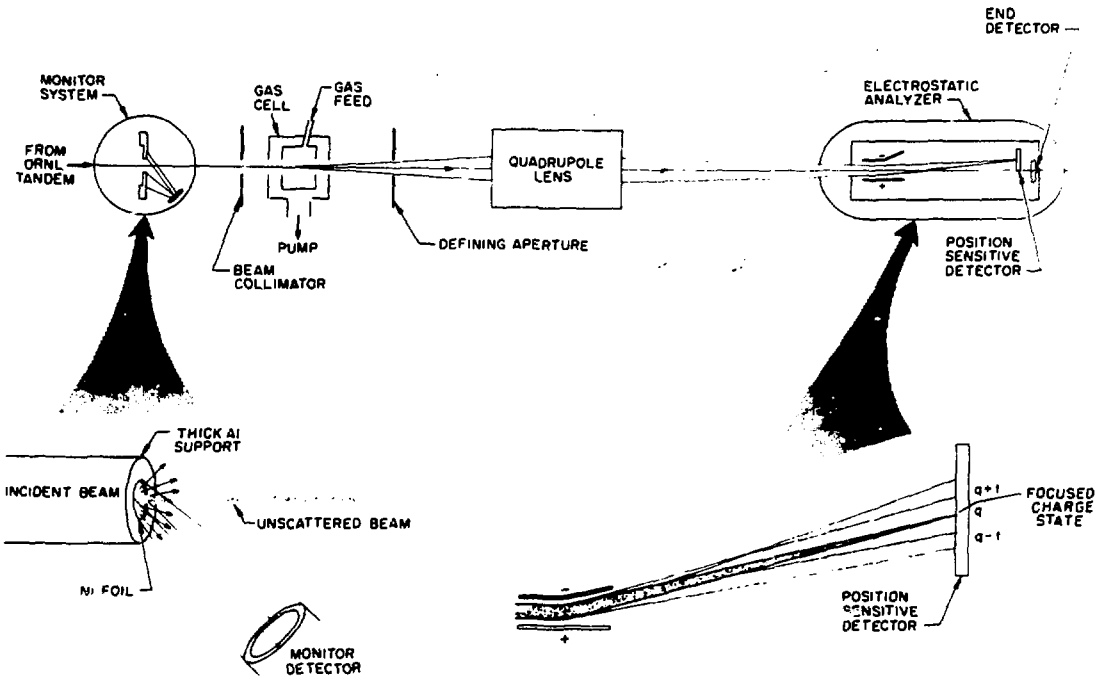

Fig. 6. Experimental arrangement for measuring total electron loss cross section (ORNL).

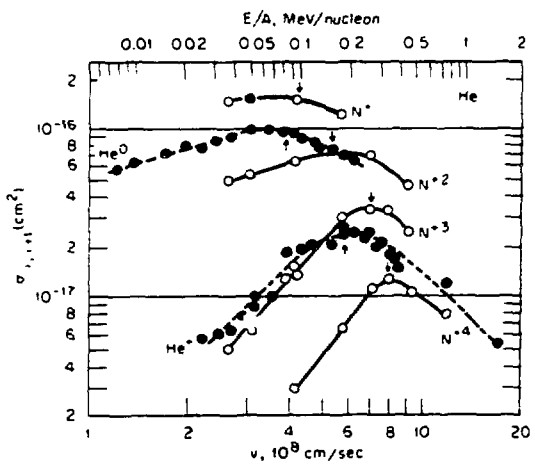

Fig. 7. Cross sections $\sigma_{i,i+1}$ for loss of a single electron for helium and nitrogen ions in helium as functions of the ion velocity, v. The arrows indicate the values $v = 1.35\ u_i$. (Nikolaev[1])

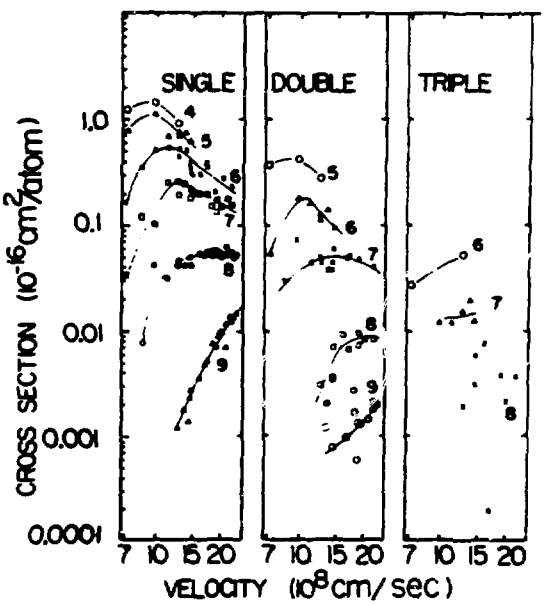

Fig. 8. Electron loss cross sections for fluorine ions on nitrogen as a function of ion velocity. (Macdonald *et al.*[15])

similiarities lead the authors to conjecture that multiple loss processes are independent of the number of electrons lost during the interaction. The shape of the loss cross section curve is then dominated by the velocity dependence of the last electron removed. Comparison of the positions of the maxima and the shape of the single and double electron loss cross sections shown in Fig. 8, illustrate this point.

Influence of Electron Binding Energy on Single Electron Loss Cross Sections. The fact that the maxima in the loss cross section versus velocity curve is related to the orbital velocity of the electron being removed, implicitly suggests the dependence of the loss process on the binding energy of the removed electron. The observed decrease in single electron loss cross section as the initial charge state of the ion is increased, also suggests the importance of the binding energy on such processes. Nikolaev[1] argues that single electron loss cross sections are related to the number of electrons in the outer subshell which have approximately the same binding energy. A plot of single electron loss cross section per shell electron is found to decrease monotonically with increasing binding energy.

The Dependence of Electron Loss on Projectile Atomic Number, Z_1. Single electron loss cross sections as a function of projectile atomic number Z_1 exhibit structure according to experimental observation as illustrated in Fig. 9 (Nikolaev[1]). All data were taken at $v_i = 2.6 \times 10^8$ cm/sec using He and N_2 target gases. Assuming that single electron loss cross sections are related to the number of electrons in the outer shell and their dependence on ionization potential, then structure in the loss cross section versus projectile atomic number Z_1 is expected, since neither quantity varies monitonically with Z_1.

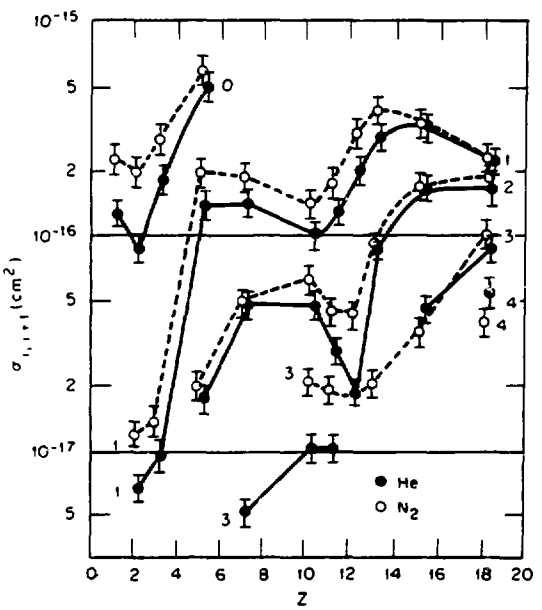

Fig. 9. The relation of the cross sections $\sigma_{i,i+1}$ for loss of a single electron to the nuclear charge Z of the ions at $v = 2.6 \times 10^2$ cm/sec in helium (•) and nitrogen (o). (Nikolaev[1])

Dependence of Loss Cross Sections on the Atomic Number of the Target, Z_2. A few investigations have been made concerning the Z_2 dependence of the loss cross sections over a wide range at targets materials (*e.g.* Nikolaev,[1] Tonuma *et al.*,[17] Knudsen *et al.*,[8] and Alton *et al.*[18]). Single electron loss cross sections versus Z_2 data of Nikolaev for helium ions ($v = 4.1 \times 10^8$ and 7×10^8 cm/sec) and ieon ions ($v = 4.1 \times 10^8$ and 5.6×10^8 cm/sec) in targets with atomic numbers ranging between $1 \leq Z_2 \leq 36$. These data, shown in Fig. 10, increase monotonically between $1 \leq Z_2 \leq 18$ but exhibit a depression between $18 \leq Z_2 \leq 36$. The suggestion by Nikolaev that the depression may be due to the effect of target polarizability seems plausible since the static polarizability of noble gases is not a monotonically increasing function of Z_2. Dynamic polarization effects which take place in such interactions may explain this effect. If so, then theoretical calculations need to include polarization potentials in order to more correctly describe these collisional processes. Effects due to polarization of the target during the interaction, are expected to increase with increasing charge of the incident ion and to decrease with increasing ion velocity. Similiar effects have been observed by Alton *et al.*[18] (Fig. 11).

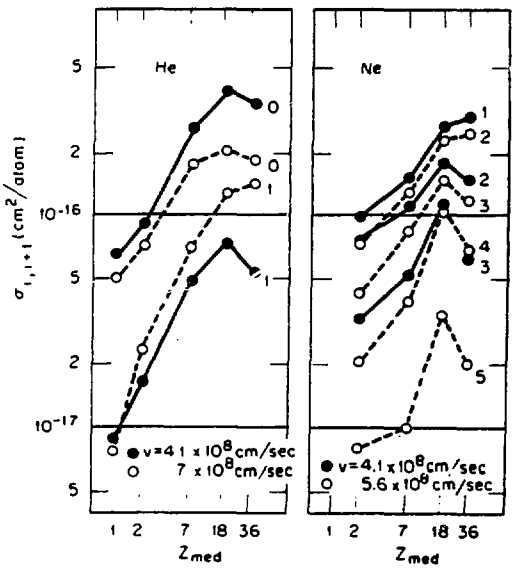

Fig. 10. The relation of the cross section $\sigma_{i,i+1}$ for loss of one electron to the atomic number Z_{med} of the medium for atoms and ions of helium and neon. The charge of the ions is indicated next to the curves. (Nikolaev[1])

Non-additivity and Density Molecular Target Effects. It has been well-known for a number of years that single electron loss cross sections per molecule for molecular targets are less than would be expected if the constituent cross sections derived from each of the individual atoms were added together, thus the term non-additivity has been used to describe this phenomenon. The effect is not surprising when a cursory analysis is made, taking into account the facts that the atoms in a molecule lie close to each other and that single electron loss collisions involve rather large impact parameters. Experimentally determined electron loss cross sections are essentially averages over all molecular orientations and impact parameters. The total annular impact parameter area associated with a given

atom of the molecule is not available for contribution to the single electron loss cross section. The net result is that the single electron loss cross section per molecule is less than the sum of cross sections from the individual constituents, *i.e.* $\sigma_{q\to q+1}/\text{mol} < \Sigma\sigma_{q\to q+1}/\text{atom}$. However, non-additivity effects are only present for large impact parameter collisions and loss of a few electrons and are usually smaller for lighter and less complex molecular targets.

Density effects involving low impact parameters and often multiple collisions are also characteristic of molecular targets. Because of non-additivity and density effects, one does not know the atomic number per atom of the target and therefore data as a function of the atomic number of molecular targets cannot be compared with those from atomic targets.

A prescription for estimating what is termed the mean atomic number per atom with which the target appears to act during interactions between 20 MeV Fe^{4+} ions and various molecular targets which result in single electron loss has been deduced by Alton[27] from the single electron loss atomic data. The formula allows one to estimate $\bar{Z}_2/n$ and is given by

$$\frac{n}{\bar{Z}_2} = \frac{1}{\Sigma z_i} \qquad (1)$$

where the sum extends over all constituents in the molecule. Expression (1) is defined as the harmonic mean of the atomic number per molecular constituent. An expression which yields almost the same result except in the case where the z_i widely differ is the arithmetic mean atomic number per constituent or

$$\frac{\bar{Z}_2}{n} = \frac{\Sigma z_i}{n^2} . \qquad (2)$$

Single electron loss cross sections per atom for interactions between 20 MeV Fe^{4+} and molecular targets can be estimated by using expression (1) in conjunction with the single electron loss cross section curve of Fig. 11 and noting the ordinate value or single electron loss cross section. This technique appears to allow the determination of single electron loss cross sections from yet unmeasured complex molecular targets. A plot of measured single electron loss cross sections per atom versus the mean atomic number per atomic constituent as calculated from expression (1) is shown in Fig. 12. We note that all measured molecular target data increase monotonically with $\bar{Z}_2/n$ and fall along a curve which passes through the noble gas atomic data.

The solid line in Fig. 12 is computed from a modified Bohr formula (see discussions below and in reference 18). We note the theoretical curve departs from the measured values at a $\bar{Z}_2/n$ of <10. This is expected since the formula was developed by Bohr[23] for heavy ion-heavy target interactions.

Non-additivity and Density Effects. The electron loss cross section per atom data versus final projectile charge state measured by Alton *et al.*[18] for interactions between 20 MeV Fe^{4+} and molecular targets Ne, CO_2, CF_4, and SF_6 illustrate non-additivity effects for $5 \leq q \leq 8$ and density effects for $q > 8$. The final charge state $q = 8$ corresponds to the argon-like electronic configuration. A gradual transition occurs between the two effects with number of electrons removed. These data indicate implicitly, a decrease in impact parameter as q increases. Projectile penetration of the molecule

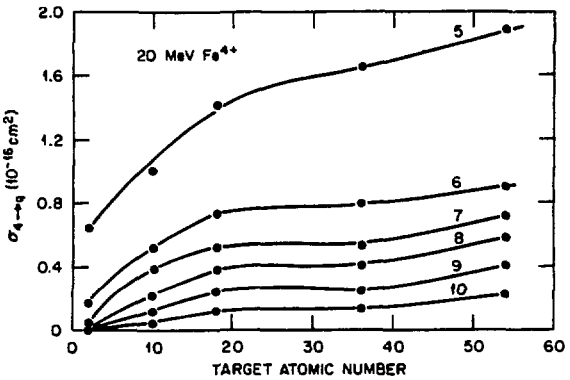

Fig. 11. Single and multiple electron loss cross section data versus atomic number for He, Ne, Ar, Kr, and Xe target gases. (Alton *et al.*[18])

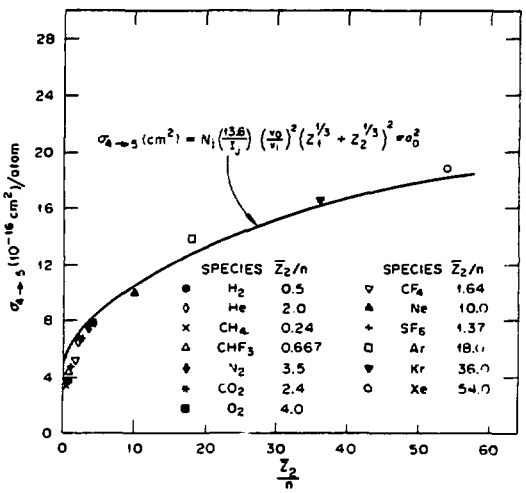

Fig. 12. Comparisons of single electron loss cross sections per atom computed from the modified Bohr formula as a function of average effective atomic number per atom with those experimentally measured. (Alton[27])

at low impact parameters may result in collisions with more than one constituent. High collision frequencies during the passage of the projectile through the molecule may enhance electron loss due to ionization and excitation in initial collisions followed by successive interactions before radiative decay takes place. This model is also used to explain differences in the charge state distributions observed for gas and solid strippers.

Shell Effects. Due to differences in electronic binding energies between subshells on either side of a closed shell (noble gas configuration), electron loss probabilities may differ significantly. Such effects have been observed many times in charge state distribution and electron capture data but have not been pronounced in electron loss cross section data according to Betz.[2] The data of Alton *et al.*[18] shown in

Fig. 13 illustrate the existence of this effect for electron loss resulting from 20 MeV Fe^{4+} interactions with the noble gases. The shell effects associated with electron removal prior and following the $1s^2 2s^2 2p^6 3s^2 3p^5$ or argon-like configuration are quite evident. Here again, unexpectedly low cross sections for Kr targets relative to those obtained from Ar and Xe for a given charge state are observed.

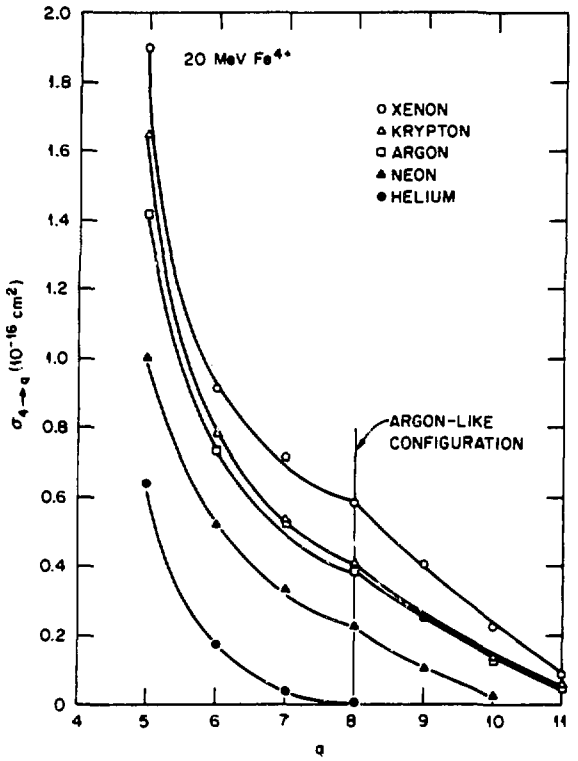

Fig. 13. Electron loss cross section versus final projectile charge state produced in He, Ne, Ar, Kr, and Xe targets. (Alton *et al.*[18])

Electron Loss Cross Section Formulas. In his 1948 treatment on the subject of particle penetration in matter, Bohr[23] deduced a formula for estimating single electron capture and loss cross sections which is assumed appropriate for fast heavy ion-heavy atom interpenetrating collisions. Knudsen *et al.*[8] have shown by comparison with experimental data that the Bohr formula given by

$$\sigma_{Bohr}(cm^2) = \pi a_o^2 \, (Z_1^{1/3} + Z_2^{1/3})^2 \, (\frac{v_o}{v_i})^2 \qquad (3)$$

agrees reasonably well in shape, but over predicts significantly, single electron loss cross sections for 20 MeV Fe^{4+} on N_2, Ar, Kr, Xe, and SF_6 targets. (In expression (3) a_o is the radius of the first Bohr orbital, Z_1, Z_2 are the atomic numbers of the projectile and target, respectively, and v_i is the velocity of the projectile.) The Bohr formula was intended at best to be a rough estimator of the cross sections for single electron capture or loss during collisions between fast heavy ion and heavy target materials, and it is not at all surprising that cross section values do not agree with those experimentally observed. On the other hand, the agreement in shape as found by Knudsen *et al.*[8] predicted by the formula is quite encouraging. The formula does not include the effects of electronic binding energies on loss processes and therefore, expression (3) should be more appropriate for more weakly bound electrons than those considered by Knudsen *et al.*

Plausible arguments can be made that cross sections for single electron loss should be directly proportional to the number of electrons residing in a given subshell N_j where the individual electronic binding energies are approximately equal. (Such arguments have also been made by Nikolaev.[1]) In this case, all electrons have equal probabilities for removal. Furthermore, one can argue that the probability of removal of a particular electron should be inversely proportional to the energy required for removal — *i.e.* the binding or ionization energy I_j of the electron. Using these arguments and the Bohr formula (expression (3)), Alton *et al.*[18] have deduced a modified single electron loss cross section formula which should be more appropriate for more tightly bound electrons. The modified formula is given by

$$\sigma_{q\to q+1}(cm^2/atom = N_j \, (\frac{13.6(eV)}{I_j(eV)}) (\frac{v_o}{v_i})^2 \times (Z_1^{1/3} + Z_2^{1/3})^2 \, \pi a_o^2 \qquad (4)$$

where the quantity 13.6 is the ionizational potential of the hydrogen atom.

Expression (4) was tested by comparing the computed results with measured single electron loss cross section data. The solid line shown in Fig. 12 was computed by use of Eq. (4) with $Z_2 \to \bar{Z}_2/n$. The authors indicate the need for further experimental measurements with other projectile charge states in order to validate these arguments.

A more general version of expression (5) has been deduced by Alton[27] which predicts single and multiple electron loss cross sections between closed shell configurations. The formula is

$$\sigma_{q_i\to q}\,(cm^2)/atom \cong \frac{13.6}{\Sigma I_j}\,(q-1)(Z_1^{1/3} + Z_2^{1/3})^2 \times (\frac{v_o}{v_i})^2 \, \pi a_o^2 \qquad (5)$$

where ΣI_j extends over all ionization potentials taken sequentially, *i.e.* the amount of energy required to remove the electrons to the continuum is equivalent to the sum of energies required for sequential ejection, q is the final charge state projectile and the other qualities have been defined previously. Expressions (4) and (5) are equivalent for the case $N_j = 4$ for single electron loss.

Expression (5) has been tested against several sets of experimental data taken from the literature involving different projectiles at equivalent velocities (8.3×10^8 cm/sec). Table 1 and 2 compare the results from expression (5) and the data of Angert *et al.*[28] and Alton *et al.*[18] for the cases indicated. (For molecular target, it is necessary to use the effective target atomic number given by expression (1) in either of formulas (4) or (5) for calculating loss cross sections per atom.)

Table 1

Test of Equation (5)
Data: Angert *et al.*[26]
Projectile: 46 MeV I^{q_i+}
Target: N_2

$q_i \rightarrow q_f$	σ_{calc} (10^{-17} cm^2)	σ_{meas} (10^{-17} cm^2)
9 → 10	15.5	18.4
10 → 11	15.1	13.2
11 → 12	14.7	18.0
12 → 13	14.4	14.0
9 → 11	8.1	12.0
11 → 13	7.6	4.2
10 → 13	5.3	6.3
12 → 14	7.4	4.5
9 → 13	5.6	6.9
10 → 12	7.8	8.9
11 → 14	5.2	7.0
12 → 15	5.1	3.3
11 → 15	4.0	4.2
12 → 16	3.9	2.1
10 → 15	3.4	1.2
11 → 16	3.3	2.2

Table 2

Test of Equation (4)
Data: Alton *et al.*[18]
Projectile: 26 MeV Fe^{4+}
Target: Ar

$q_i \rightarrow q_f$	σ_{calc} (10^{-17} cm^2)	σ_{meas} (10^{-17} cm^2)
TARGET: Ne		
4 → 5	10.5	10.0
4 6	5.7	5.2
4 7	4.1	3.4
4 8	3.2	2.2
TARGET: Ar		
4 5	12.5	14.2
4 6	6.8	7.3
4 7	4.8	5.2
4 8	3.8	4.0
TARGET: Xe		
4 5	18.2	19.0
4 6	9.9	9.2
4 7	7.0	7.1
4 8	5.5	5.9

Conclusions

From the studies of electron loss processes which occur in high energy heavy ion target interactions which have been made to date, many interesting and important aspects of these processes have been discovered which has led to a broader understanding of the energy transfer mechanisms involved. Several examples, shown in the text, illustrate some of the effects which are characteristic of these loss processes. Although several studies have been made and a significant data base has been established from which general trends or expected effects can be estimated, it is clear that more studies need to be made. For example, few velocity dependent measurements have been made involving the loss of large numbers of electrons and few scattering experiments have been conducted at these projectile energies from which more detailed understanding of the dynamics involved in such collisions can be obtained. The results from such experiments can be used to develop realistic interaction potentials by comparing observation with theory. It is clear that the data base should be extended by including many more projectiles, projectile energies, and initial charge states, etc. so that sufficient data is available for developing an adequate theory for these interactions. Such theories do not exist for description of these complex processes.

Acknowledgements

I would like to acknowledge with gratitude the contributions of other members of the Oak Ridge National Laboratory based research group which include: Drs. C. D. Moak, P. D. Miller, C. M. Jones from the Oak Ridge National Laboratory; Q. C. Kessel and A. Antar from the University of Connecticut; and L. B. Bridwell from Murray State University. Also the skillful typing of Ms. Lynda Hawkins is sincerely appreciated.

References

1. V. S. Nikolaev, Soviet Physics USPEKHI 8, 269 (1965).
2. H. D. Betz, Rev. Modern Phys. 44, 465 (1972).
3. C. D. Moak, IEEE Trans. Nucl. Sci. NS-19, No. 2, 243 (1972).
4. C. D. Moak, IEEE Trans. Nucl. Sci. NS-23, No. 2, 1126 (1976).
5. S. Datz, C. D. Moak, H. O. Lutz, L. C. Northcliffe, and L. B. Bridwell, Atomic Data 2, 273 (1971).
6. G. D. Alton, J. A. Biggerstaff, L. B. Bridwell, C. M. Jones, Q. C. Kessel, P. D. Miller, C. D. Moak, and B. Wehring, IEEE Trans. Nucl. Sci. NS-22, 1685 (1975).
7. C. D. Moak, L. B. Bridwell, H. A. Scott, G. D. Alton, C. M. Jones, P. D. Miller, R. O. Sayer, Q. C. Kessel, and A. Antar, Nucl. Instrum. and Methods 150, 529 (1978).
8. H. Knudsen, C. D. Moak, C. M. Jones, P. D. Miller, R. O. Sayer, G. D. Alton, and L. B. Bridwell, Phys. Rev. A19, 1029 (1979).
9. V. S. Nikolaev and I. S. Dmitriev, Phys. Letters 28A, 277 (1968).
10. R. O. Sayer, Revue de Physique Applique 12, 1543 (1977).
11. S. K. Allison, Rev. Mod. Phys. 30, 1137 (1958).

12. S. K. Allison and M. Garcia-Munoz, in Atomic and Molecular Process, edited by D. R. Bates (Academic, New York, 1962), p. 721.

13. L. C. Northcliffe, Ann. Rev. Nucl. Sci. 13, 67 (1963).

14. J. R. Macdonald and F. W. Martin, Phys. Rev. A4, 1965 (1971).

15. J. R. Macdonald, S. M. Ferguson, T. Chiao, L. D. Ellsworth, and S. A. Savoy, Phys. Rev. 5, 1188 (1972).

16. S. M. Ferguson, J. R. Macdonald, T. Chiao, L. D. Ellsworth, and S. A. Savoy, Phys. Rev. 8, 2417 (1973).

17. T. Tonuma, I. Kohno, Y. Miyazawa, F. Yoshida, T. Karasawa, T. Takahashi, and S. Konno, J. Phys. Soc. of Japan 34, 148 (1973).

18. G. D. Alton, L. B. Bridwell, M. Lucas, C. D. Moak, P. D. Miller, C. M. Jones, Q. C. Kessel, A. A. Antar, and M. D. Brown (accepted for publication in Phys. Rev. A)

19. Q. C. Kessel, Phys. Rev. A5, 1881 (1970).

20. R. A. Spicuzza and Q. C. Kessel, Phys. Rev. A14, 630 (1976).

21. L. B. Bridwell, J. A. Biggerstaff, G. D. Alton, C. M. Jones, P. D. Miller, Q. Kessel, and B. Wehring, *4th Intl. Conf. on Beam Foil Spectroscopy*, Sept. 15-19, Gatlinburg, TN.

22. H. A. Scott, L. B. Bridwell, C. D. Moak, G. D. Alton, C. M. Jones, P. D. Miller, R. O. Sayer, Q. C. Kessel, and A. Antar, Phys. Rev. A18, 2459 (1978).

23. N. Bohr, Kgl. Danske Videnskab. Selskab. Mat.-Fys. Medd. 18, No. 8 (1948).

24. N. Bohr and J. Lindhard, Kgl. Danske Videnskab. Selskab. Mat.-Fys. Medd. 28, No. 7 (1954).

25. R. Ryding, A. Wittkower, and P. H. Rose, Phys. Rev. A3, 1658 (1971).

26. Q. C. Kessel, Rev. Sci. Instr. 40, 68 (1969).

27. G. D. Alton (unpublished).